Journal of materials and Environmental Sciences
ISSN : 2028-2508

JMES, 2017 Volume 8, Issue 2, Page 426-437

http://www.jmaterenvironsci.co

Efficient removal of Ni^{2+} ions from aqueous solution using activated carbons fabricated from rice straw and tea waste

V.T. Tran[1], D.T. Nguyen[1], V.T.T. Ho[2], P. Q. H. Hoang[3], P.Q Bui[1], L.G. Bach[1]

[1]*NTT Institute of High Technology, Nguyen Tat Thanh University, Ho Chi Minh City, Vietnam*
[2] *Hochiminh City University of Natural Resources and Environment, Ho Chi Minh City, Vietnam*
[3]*Faculty of Biotechnology and Environmental Engineering, HCMC University of Food Industry, Vietnam*

Received 16 Jun 2016,
Revised 23 Nov 2016,
Accepted 10 Dec 2016

Keywords

- ✓ Ni^{2+} contamination;
- ✓ KOH;
- ✓ activated carbons;
- ✓ rice straw;
- ✓ tea waste;
- ✓ agricultural waste.

blgiangntt@gmail.com
+84839405875

Abstract

The removal of Ni2+ in aqueous solution was investigated by adsorption process on activated carbons fabricated from rice straw (RSAC) and tea waste (TWAC). The samples were characterized by XRD, SEM, N2 adsorption (BET), and TGA. The response surface methodology was employed to optimize the maximum percentage of Ni2+ removal. The results showed that the surface area of TWAC was about four times greater than that of RSAC and thus the TWAC exhibited higher adsorption capacity for Ni^{2+}. The adsorption isotherms were also evaluated by Langmuir, Freundlich and Temkin equations revealed that both monolayer and multilayer adsorption were effective in the uptake process of metal ions. By the optimization using the *RSM*–based quadratic regression equations, the impact of independent variables including metal ion concentration, pH and AC dosage on the removal of Ni^{2+} was statistically investigated

1. Introduction

Nickel is an essential microelement not only for living organisms but also for the manufacturing of various kinds of alloys and electroplating industry. Nevertheless, the presence of nickel in water causes toxic effects on human health. It has been reported that long–term uptake of nickel contaminated drinking water has infected diseases such as vomiting, chest pain, and rapid respiration. Thus, The World Health Organization (WHO) provisional guideline of 0.02 ppm has been restricted as the drinking water standard.[1]

Several treatment techniques were commonly applied to eliminate Ni^{2+} from an aqueous solution such as ion exchange, chemical precipitation, ultrafiltration, electro–chemical deposition and adsorption [2–4]. It is documented that adsorption process employed activated carbon (AC) as a highly efficient adsorbent is proved to be a promising method due to its emergent characteristics, such as high porosity, large surface area and diverse functional groups on the surface.

In recent years, the fabrication of agricultural waste–derived AC has paid much attention. As a comparison to commercial activated carbons, agricultural waste–derived AC can be prepared from the widespread and zero–cost source while the quality of products is equivalent. Many researchers have reported the facilities of transforming from a variety of non–toxic and renewable agricultural wastes, such as tea waste, rice husk, sugarcane bagasse, banana peels, etc. into low–cost and high–performance AC [5–8]. Accordingly, taking advantage of raw materials for the fabrication of AC can not only reduce the disposal of untreated wastes but also increase the efficient use of carbonaceous source instead for the uneconomical purposes as combustion and organic fertilizers.

Normally, AC can prepare by two processes is that physical and chemical activation. The first method can accomplish by one–pot direct synthesis route in the presence of CO_2 or steam [7]. The remaining method can be achieved by two steps: (1) the raw material is impregnated with strong dehydrating reagents such as KOH, $ZnCl_2$, K_2CO_3, and H_3PO_4; (2) chemical–impregnated material is then pyrolyzed to develop new pore structure through the oxidative reactions between carbon atoms and reagent molecules [7,9–11]. Among the aforementioned methods, the chemical activation received much attention due to the following reasons: (i) as comparison with the physical process, the chemical activation process takes place at a lower temperature and

shorter time needed for activating material; (ii) ACs prepared by the chemical activation process shown very high surface area; (iii) the yields of ACs in chemical activation are usually higher than in physical activation process because dehydrating reagents can inhibit formation of tar and reduce the production of other volatile products [12–14]. Besides, it is well–known that KOH is widely used as an efficient chemical in the preparation of AC from lignocellulosic products because of its eco–friendly and non–polluting character [2]. The present work aims to fabricate ACs from rice straw and tea waste by chemical activation with KOH as the activating agent. We also investigated the Ni^{2+} adsorption kinetics of the as–prepared ACs with identifying the optimal conditions (initial Ni^{2+} concentration, the dosage of ACs and pH of the solution) required to maximize the removal efficiency of Ni^{2+}.

2. Materials and methods

2.1. Production of ACs

All chemicals for this study were commercially purchased from Merck and used as received without any further purification. We prepared ACs samples from rice straw and tea waste by chemical activation with KOH as the activating agent. Typically, all raw materials were firstly pretreated by heating at 105 ^oC for 3 h. The dried raw material (rice straw or tea waste) was carbonized at 500 ^oC (with a heating rate of 10 ^oC/min) for 60 min in N_2 flow (with a flowing rate of 400 cm^3/min). The residual char then was soaked with KOH solution (KOH/Char weight ratio of 1) for 1 day before heated to 800 ^oC using the same given system during 60 min. All samples were repeatedly washed with deionized water until filtered water obtained a neutral solution. Finally, the as–synthesized ACs were slowly dried at 105^oC for 24 h. ACs prepared from the rice straw and tea waste were noted RSAC and TWAC, respectively. The formation yields of ACs were calculated: 28 % and 31 % for RSAC and TWAC samples, respectively.

2.2. Characterization of the as–prepared ACs

The X–ray powder diffraction (XRD) of ACs was implemented on D8 Advance Bruker powder diffractometer with a Cu–Kα excitation source and a scan rate of 0.02^o/s from 0^o to 50^o. The scanning electron microscope (SEM) was recorded by instrument S4800, Japan and used an accelerating voltage source of 10 kV with a magnification of 7000. The FT–IR spectra were recorded by using the Nicolet 6700 spectrophotometer instrument. The N_2 adsorption/desorption isotherm was obtained using the Micromeritics 2020 volumetric adsorption analyzer system. BET surface area was measured using the isotherm equation. The thermal decomposition of activated carbons in N_2 atmosphere was carried out on a TGA Q500 Universal V4.5A instrument. The samples were positioned in a platinum plate and degassed in vacuum in prior to use. The experiments were then performed beneath N_2 atmosphere (40 cm^3/min, 10^{o}C/min) from room temperature to 900 ^oC. Because TGA was conducted in N_2 atmosphere so we suggested that pyrolysis is suitable to describe the thermal decomposition process.

2.3. Adsorption batch

The as–prepared ACs (0.8 g/L – 9.2 g/L) was poured in an Erlenmeyer flask containing 50 mL of Ni^{2+} aqueous solution (8 ppm – 92 ppm). After absorption equilibrium obtained, the adsorbent was removed from the mixture using filter paper. The residual concentrations were confirmed by AAS and Ni^{2+} removal was calculated by the following equation:

$$Ni^{2+}\ removal\ (\%) = \frac{C_o - C_f}{C_o}.100 \qquad (1)$$

where, C_o and C_e are initial and equilibrium Ni^{2+} concentrations (ppm), respectively. The Ni^{2+} uptake was calculated as follows:

$$q_e\ (mg/g) = \frac{C_o - C_e}{W}.V \qquad (2)$$

where, V is the volume of the Ni^{2+} solution (mL) and W is the weight of adsorbent (g).

2.4. Experimental design with response surface methodology (RSM)

Herein, RSM technique is used to optimize experimental results through second order polynomial regression equations, which describe the true mathematical relationship between response (y) and the set of independent values (x) as following equation:

$$y = f(x) = \beta_o + \sum_{i=1}^{k}\beta_i x_i + \sum_{i=1}^{k}\sum_{j=1}^{k}\beta_{ij} x_i x_j + \sum_{i=1}^{k}\beta_{ii} x_i^2 \qquad (3)$$

where, y is the predicted response; x_i and x_j are the independent variables (i,j=1, 2, 3, 4….k). The parameter β_o is the model constant; β_i is the linear coefficient; β_{ii} is the second–order coefficient and β_{ij} is the interaction coefficient. Among the experimental matrix designs, central composite design (CCD) is recognized as one of the most popular techniques of quadratic designs, which random experimentation was established without employing a large number of experiment runs (Table 1). Accordingly, the center variables (encoded 0) are utilized to determine the experimental error and the reproducibility of the data. The margin points including the low (encoded –1), high (encoded +1) and rotatable (encoded ±α) levels are also manipulated. Therefore, as a total number of experiments (N) for three independent variables (k = 3) including the 2^k factorial experiments, 2k axial experiments and six replication is 20. Analysis of variance (ANOVA) is calculated using Design–Expert version 9.0.5.1 (DX9). ANOVA of the quadratic polynomial regression model from is utilized to identify the signification of input variables and output variables as well as the relationship between the responses and the independent factors.

2.5. Adsorption isotherms

For adsorption isotherm experiments, 5.0 g/L rice straw– and tea waste–derived AC samples was poured into an Erlenmeyer flask containing 50 mL of Ni^{2+} aqueous solution of different concentration (8.0 ppm – 92.0 ppm) at pH = 4. All tests were herein employed at room temperature until absorption equilibrium obtained completely.

Langmuir isotherm equations: The monolayer adsorption is described by Langmuir model, which assumes the adsorption behavior occurs on a homogeneous surface with a finite number of adsorption sites, expressed as follows:

$$\frac{1}{q_e} = \left(\frac{1}{q_m K_L}\right).\frac{1}{C_e} + \frac{1}{q_m} \qquad (3)$$

where, C_e (mg/L) and q_e (mg/g) are equilibrium concentration and adsorption capacity, respectively. q_m (mg/g) and K_L (L/mg) are the maximum adsorption capacity and rate of adsorption (Langmuir constant), respectively. Term of constant separation factor (R_L) is one of the essential dimensionless equilibrium parameters of the Langmuir isotherm modeling, which is defined by the following equation:

$$R_L = \frac{1}{1 + K_L C_o} \qquad (4)$$

where: K_L (L/mg) is the Langmuir constant and C_o (mg/L) is the highest metal ions concentration. The types of the R_L value–based isotherm is determined as follows: $0 < R_L < 1$ presents a favorable adsorption process; however, an $R_L > 1$ is considered as an unfavorable process. Alternatively, adsorption isotherm is linear or irreversible if the value of R_L is found to be 1 and 0, respectively.

Freundlich isotherm equations: The Freundlich model is used for the description of non–ideal sorption on heterogeneous surfaces and multilayer adsorption processes based on the interaction between adsorbed molecules at different energies. The Freundlich isotherm model assumes the relationship between non–ideal and reversible adsorption, which is an empirical equation as follow:

$$\ln q_e = \ln K_F + \frac{1}{n}\ln C_e \qquad (5)$$

where: *1/n* and K_F [(mg/g).(L/mg)$^{1/n}$] are Freundlich constants related to the favorability of adsorption process and the adsorption capacity of the adsorbent, respectively.

The slope (value of 1/n) ranges between 0 and 1 is a means of adsorption intensity or surface heterogeneity. As the value of the slope approaches zero, the more heterogeneous of the process, whereas a value below unity implies chemisorption's process. A slope above the value of one indicates a cooperative adsorption (the physical process).

Temkin isotherm equations: Temkin model is represented by the following equation:

$$q_e = B_1 \ln K_t + B_1 \ln C_e \quad (6)$$

where, $B_1 = \frac{RT}{b}$. K_t (L/g) and b (J/mol) are the Temkin equilibrium constant (L/mol) and constant B_1 is related to the heat of adsorption, respectively. R is a gas constant of 8.314 (J.mol^{-1}K^{-1}).

3. Results and discussion

3.1 Characterization of activated carbon

The structure of AC derived from rice straw and tea waste was first characterized by means of XRD analysis, as shown in Figure 1. In Figure 1, the presence of typical broad peaks in the 2θ range from 20° to 30° (RSAC) or

from 10^{o} to 20^{o} (TWAC) demonstrated both AC samples possess the amorphous structure. Moreover, the absence of sharp peaks indicated the negligible existence of residual ash and metal trace in the structure.

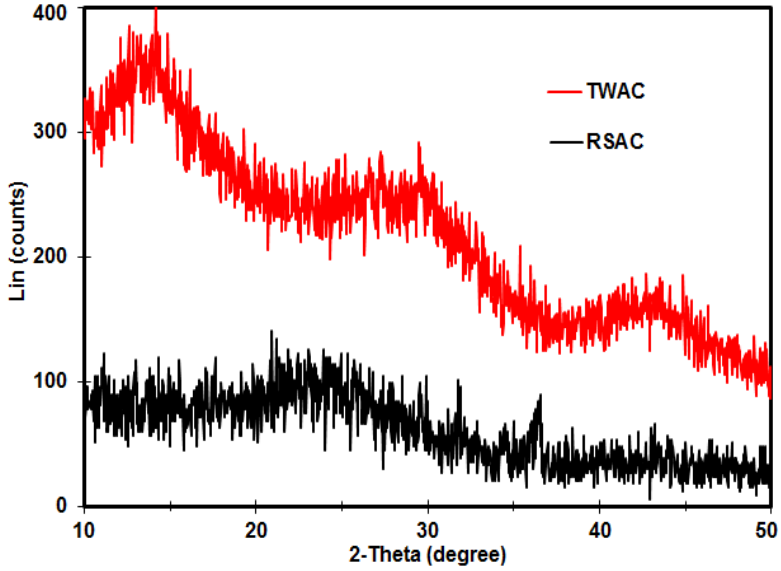

Figure 1: XRD spectra of the ACs.

Figure 2 compared the FT–IR spectra of the as–synthesized AC from rice straw (RSAC) and tea waste (TWAC). Generally, both samples were similarly found to be a complex surface which consisted various kinds of functional groups. The strong absorption band around 3450 cm^{-1}, visible for all samples, was attributed to the O–H stretching vibrations, hydroxyl groups and adsorbed water.[15] According to the literature, KOH was represented as strong hydrolysis agent, which can break aliphatic and aromatic bonding species of cellulose structure to form novel bonds [4]. This phenomenon can be explained by the presence of the O–N asymmetric stretch (1541 cm^{-1}), C≡C bonding (2353 cm^{-1}), olefinic C=C vibrations (1640 cm^{-1}) and aliphatic C–H stretching (2916 cm^{-1}). Besides, the strong band seen at 1082 cm^{-1} may be ascribed to the asymmetric and symmetric vibrations of C–O stretching [16].

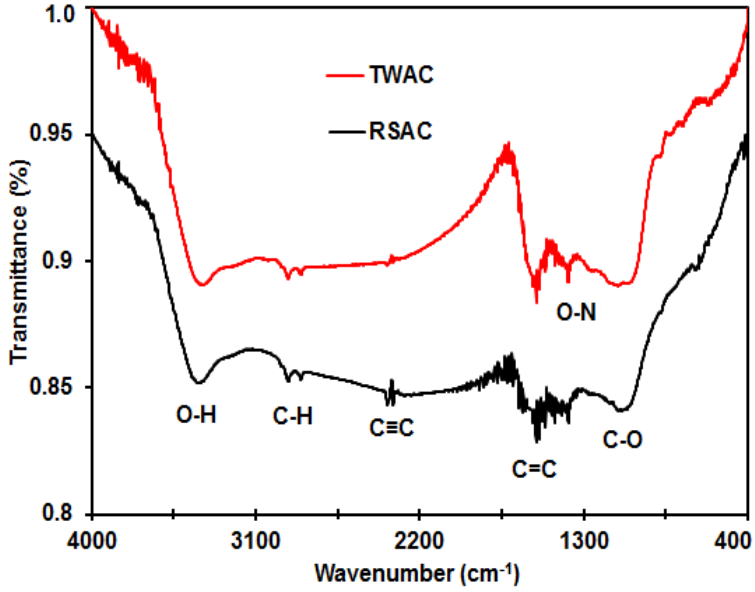

Figure 2: FT–IR spectra of the ACs.

Three stages of carbonization process of rice straw and tea waste were studied by TGA technique and displayed in Figure 3. In the low range of temperature (50 ^{o}C–200 ^{o}C), preliminary emission of volatile components for example water and other impurities accounts for a small loss of 10 % weight. According to our best knowledge, main component of raw materials comprises hemicellulose, cellulose, and lignin. In the higher temperature (200 ^{o}C–500 ^{o}C), the pyrolysis occurred strongly with a decrease of 50 % corresponding to the decomposition of cellulose and hemicellulose (200 ^{o}C < T < 370 ^{o}C). The final stage was observed loss of 30 % by the thermal decomposition of lignin (375 ^{o}C < T < 650 ^{o}C) [12, 17, 18]. Generally, pyrolysis of main components

completely occurred at around 600°C. Based on these analyses, and hence, activation temperature for the fabrication of AC was chosen to employ at 600 °C.

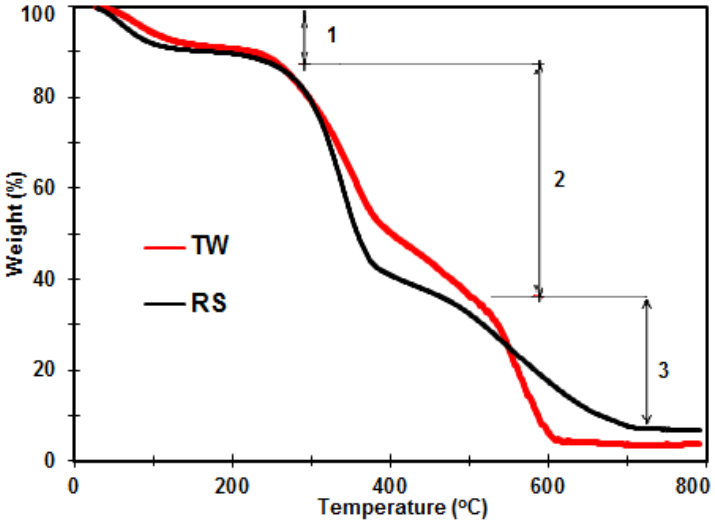

Figure 3: TGA analysis of the raw materials.

The effects of various raw material sources on the pore size distribution and BET surface area of AC were observed. The average micro–pores radius of RSAC TWAC were found to be 7.9 Å and 5.8 Å (Figure 4). While, the BET surface area based on the measurement of N_2 adsorption/desorption isotherm reveals surprisingly different results, 253.8 m^2/g (RSAC) versus 1107.6 m^2/g (TWAC). Such difference in textural structure of the two kinds of activated carbons could be attributed to various original constitutes of raw materials which induced formation of pore system during carbonization. Note that tea waste contains cellulose (37%), hemicellulose and lignin (14%) and polyphenol (25%) and tannins [19] while rice straw is composed of cellulose (33.35%), hemicellulose (31.42%) and lignin (4.84%) [20, 21].

The properties were proved again by the observation in SEM micrographs, which reveals the surface morphology of the as–synthesized AC (Figure 5). In comparison, the structure of TWAC was observed to be more highly porous and rich–defective than RSAC. Thus, the TWAC is expected to exhibit higher adsorption performance than the RSAC.

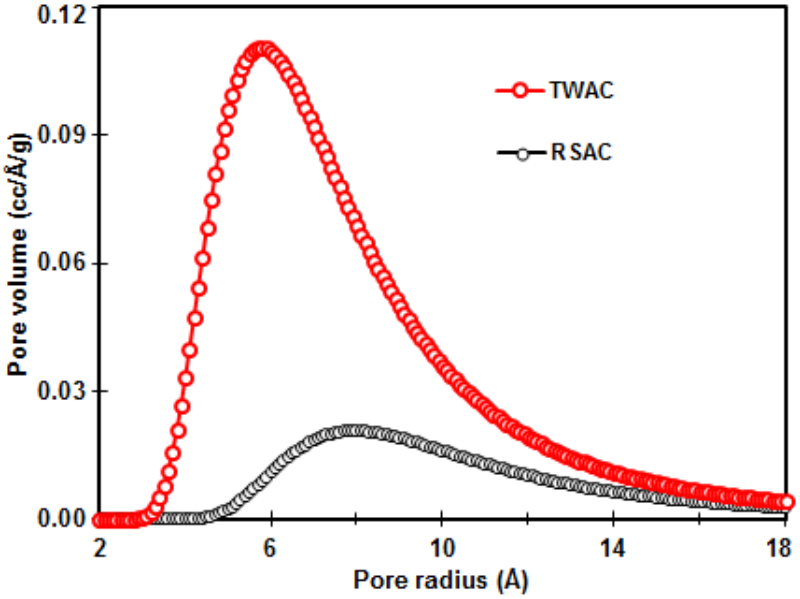

Figure 4: Pore size distribution of the ACs.

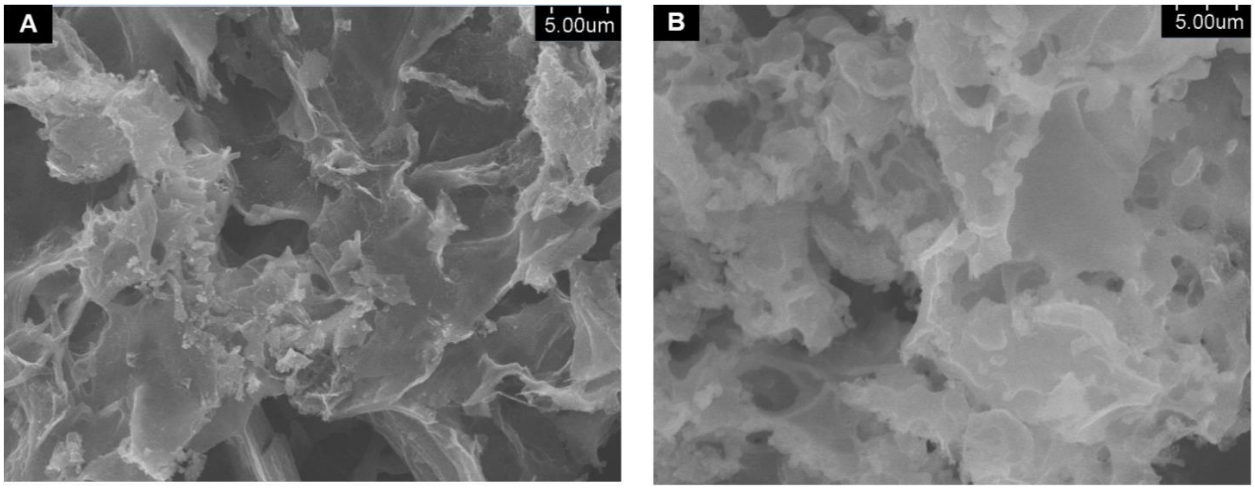

Figure 5: SEM micrographs of the RSAC (A) and TWAC (B).

3.2 Quadratic models for the removal of Ni^{2+}

To obtain the optimum models, twenty experiments were first designed according to the guide of CCD matrix. In detail, five levels of the encoded variables were defined as follows: the low (–1), high (+1), central (zero) and rotary (±α). Three independent variables including initial Ni^{2+} concentration, pH and AC dosage) were investigated to assess their effects on the main response as the percentage of Ni^{2+} removal (Table 1). Two models were otherwise established to compare the difference of Ni^{2+} removal efficiency by the use of various activated carbons. Table 2 exhibits the experimental results for Ni^{2+} of 20 runs along with the respective DX9–predicted removal results. These predicted results were derived from the regression analysis of CCD, which afforded the following second order polynomial equations for both types of activated carbon:

$$y_{RSAC} = 61.8 - 1.68x_1 + 12.68x_2 + 22.53x_3 - 3.00x_1x_2 + 0.55x_1x_3 + 01.25x_2x_3 + 0.26x_1^2 - 8.14x_2^2 - 6.56x_3^2 \quad (7)$$

$$y_{TWAC} = 92.9 - 2.34x_1 + 7.32x_2 + 26.12x_3 + 7.65x_1x_2 + 5.35x_1x_3 - 0.30x_2x_3 - 3.48x_1^2 - 17.13x_2^2 - 16.67x_3^2 \quad (8)$$

Table 1: Independent variables matrix and their encoded levels.

No	Independent factors	Code	Levels				
			$-\alpha$	–1	0	+1	$+\alpha$
1	Initial Ni^{2+} concentration (ppm)	x_1	8.0	25	50	75	92.0
2	AC dosage (g/L)	x_2	0.8	2.5	5	7.5	9.2
3	pH of solution (–)	x_3	0.6	2	4	6	7.4

Table 2 also demonstrates that Ni^{2+} removal efficiency was strongly influenced by the values of the input factors and the textural properties of activated carbons, which obtained average percentage at center points was found to be 61.8 % (RSAC) and 92.9 % (TWAC). The main contents of Table 3 include the results of the analysis of variance (ANOVA) fitted to the second–order polynomial equations and the corresponding regression coefficients. In detail, the high statistical significance of the models can be evaluated by high *F*– and low *p*–values. A *p*–value is less than 0.05 demonstrates the statistical significance of factor effect (at 95 % confidence level), while a higher *F*–value describes better fitness of proposed models. Adequate precision (AP) ratios measure the signal to noise ratios, which AP is greater than 4.0 indicating the model has an adequate signal. Moreover, determination of coefficients R^2 closer 1.0 reveals the higher accuracy of the obtained models. In particular, lack of fit (LOF) value parameters shows the variation of responses around the fitted model and this parameter appears insignificant if the model fits data well. According to these standards, Table 3 represents the high *F*–values of both models along with Prob. > F values lower than 0.0001 suggested the significance of the proposed models. Adequate precision ratios of the removal of nickel ions were 41.1 and 40.7 for RSAC and

TWAC models, respectively shows that both models can be used to navigate the design space. The values of R^2 and adjusted R^2 of two models were higher than 0.98 indicated the strong significance of models. Furthermore, the *LOF*–values were found to be more than 0.05 showed again the significant model correlation between the variables and responses. Otherwise, the modeling adequacy can also be confirmed by whether diagnostic plots of actual versus predicted data for the removal of Ni^{2+} follows a normal distribution. According to observation in Figure 6, almost observed points were closely positioned to the straight line indicating a good correlation between actual and predicted values.

Table 2: Matrix of observed and predicted values.

Run	Independent factors (encoded)			Ni^{2+} removal (%)			
				Actual values		Predicted values	
	x_1	x_2	x_3	y_{RSAC}	y_{TWAC}	y_{RSAC}	y_{TWAC}
1	25	2.5	2	10.8	37.6	12.6	37.2
2	75	2.5	2	14.7	5.9	14.2	6.5
3	25	7.5	2	38.4	37.0	41.5	37.2
4	75	7.5	2	28.5	35.5	31.0	37.1
5	25	2.5	6	54.8	77.6	54.1	79.4
6	75	2.5	6	59.1	66.9	57.9	70.1
7	25	7.5	6	85.6	75.4	88.0	78.1
8	75	7.5	6	79.7	95.7	79.7	99.4
9	8	5	4	68.4	87.9	65.4	87.0
10	92	5	4	59.3	82.9	59.7	79.1
11	50	0.8	4	16.2	33.6	17.5	32.1
12	50	9.2	4	64.0	60.0	60.1	56.8
13	50	5	0.6	8.6	1.4	5.3	1.8
14	50	5	7.4	80.5	94.8	81.1	89.7
15	50	5	4	60.6	94.3	61.8	92.9
16	50	5	4	60.0	95.1	61.8	92.9
17	50	5	4	63.2	94.7	61.8	92.9
18	50	5	4	64.6	90.3	61.8	92.9
19	50	5	4	61.6	90.9	61.8	92.9
20	50	5	4	60.4	91.2	61.8	92.9

3.3 Effect of variables on the removal efficiency of Ni^{2+}

The surface responses of the quadratic model were described using the three–dimensional curves, which one variable maintained at a central value while the others fluctuated in the experimental ranges. The effects of input variables (initial concentration, adsorbent dosage, and pH of solution) on the removal efficiency of Ni^{2+} metal ions were totally expressed in Figures 7. In detail, 3D graph shows in Figure 7A and B was developed as a function of two factors: initial concentration (8 – 92 ppm) and adsorbent dosage (0.8 – 9.2 ppm) at the constant value of pH = 4.0. According to the observation in Figures 7A, the effect of initial concentration on the removal efficiency of Ni^{2+} was unremarkable within the low value of RSAC dosage. At the greater amount of RSAC dosage, the stronger effect of initial concentration on the percentage of Ni (II) removal was observed. Ni (II) removal efficiency was increased (48 % – 70 %) by decreasing initial concentration (92 ppm – 8 ppm). On the other hand, RSAC dosage lifted from 0.8 g/L to 9.2 g/L could support the removal of Ni (II) by significant raise from 10 % to maximum 70 %. According to data in Figures 7B, the same observation was repeatedly presented

when the percentage of Ni (II) removal was strongly dependent on TWAC dosage regardless of various values of initial concentration. It was obvious that Ni^{2+} ions were almost absent from aqueous solution (94 % removal) by using optimum TWAC amount of 5.5 g/L at 50 ppm of initial concentration. The adsorption behavior of metal ions by AC can be explained due to the presence of a number of rich–electron functional groups on the material surface, which captured metal ions by coordinate bonds. When adding the greater amount of adsorbent can lead to raising the number of active sites, and hence adsorption of metal ions by this sites would enhance.

Table 3: ANOVA for response surface quadratic models.

Response	Source	Sum of squares	Degree of freedom	Mean square	F–value	Prob > F	Comment
	Model	10728.17	9	1192.02	147.53	< 0.0001 [s]	SD = 2.84
	x_1	38.41	1	38.41	4.75	0.0542 [n]	Mean = 51.95
	x_2	2196.31	1	2196.31	271.82	< 0.0001 [s]	CV (%) = 5.47
	x_3	6933.67	1	6933.67	858.13	< 0.0001 [s]	Press = 514.2
	x_1^2	72.00	1	72.00	8.91	0.0137 [s]	R^2 = 0.9925
y_{RSAC}	x_2^2	2.42	1	2.42	0.30	0.5962 [n]	$R^2_{(adj.)}$=0.9858
(%)	x_3^2	12.50	1	12.50	1.55	0.2419 [n]	AP = 41.1
	x_1x_2	0.98	1	0.98	0.12	0.7343 [n]	
	x_1x_3	953.85	1	953.85	118.05	< 0.0001 [s]	
	x_2x_3	620.60	1	620.60	76.81	< 0.0001 [s]	
	Residuals	80.80	10	8.08			
	Lack of Fit	64.35	5	12.87	3.91	0.0804 [n]	
	Pure Error	16.45	5	3.29			
	Model	18309.72	9	2034.41	176.53	< 0.0001 [s]	SD = 3.39
	x_1	75.02	1	75.02	6.51	0.0288 [s]	Mean = 67.44
	x_2	732.22	1	732.22	63.54	< 0.0001 [s]	CV (%) = 5.03
	x_3	9315.49	1	9315.49	808.33	< 0.0001 [s]	Press = 727.78
	x_1^2	468.18	1	468.18	40.63	< 0.0001 [s]	R^2 = 0.9937
y_{TWAC}	x_2^2	228.98	1	228.98	19.87	0.0012 [s]	$R^2_{(adj.)}$ = 0.9881
(%)	x_3^2	0.72	1	0.72	0.062	0.8077 [n]	AP = 40.7
	x_1x_2	174.37	1	174.37	15.13	0.0030 [s]	
	x_1x_3	4226.65	1	4226.65	366.76	< 0.0001 [s]	
	x_2x_3	4002.82	1	4002.82	347.33	< 0.0001 [s]	
	Residuals	115.24	10	11.52			
	Lack of Fit	91.69	5	18.34	3.89	0.0811 [n]	
	Pure Error	23.55	5	4.71			

Note: [s] significant at $p < 0.05$, [n] insignificant at $p > 0.05$. x_1, x_2 and x_3 are the main factors. x_1^2, x_2^2 and x_3^2 are the square factors. x_1x_2, x_1x_3 and x_2x_3 are the interaction factors.

The surface response plots in Figure 7C and D reveals the effect of initial concentration (8 ppm – 92 ppm), pH of the solution (0.6–7.4) and AC dosage of 5.0 g/L on the Ni^{2+} removal. According to observation in both Figure 7C and 7D, it was generally found that the removal efficiency was only dependent on the pH of the solution while the influence of initial concentration was nearly zero despite a widespread range of *pH*–values. The removal of Ni^{2+} ions was unfavorable in strongly acidic solution (pH < 2) regardless of any variation values of initial concentration. This phenomenon can be explained due to the presence of H^+ ions extremely prohibited the formation of coordinate bonds between metal ions and rich–electron active sites. When decreasing the density of proton in solution to reach a neutral environment could facilitate the adsorption of Ni^{2+}. In that cases, the appropriate *pH*–values were found to be 7.0 and 6.0 for the maximum removal experiments of Ni^{2+} by RSAC

(83 %) and TWAC (100 %), respectively. When *pH*–values were more than 8.0, a highly basic aqueous solution could form hydroxide–metal precipitation. Hence, the measurement of Ni^{2+} removal using solid adsorbents can be inappropriate because of the existence of chemical precipitation. Present results were also a good agreement with several previous studies, which reported the range of optimum *pH*–value for adsorption of Ni^{2+} ions was found to be 6.0 – 6.5 [22, 23].

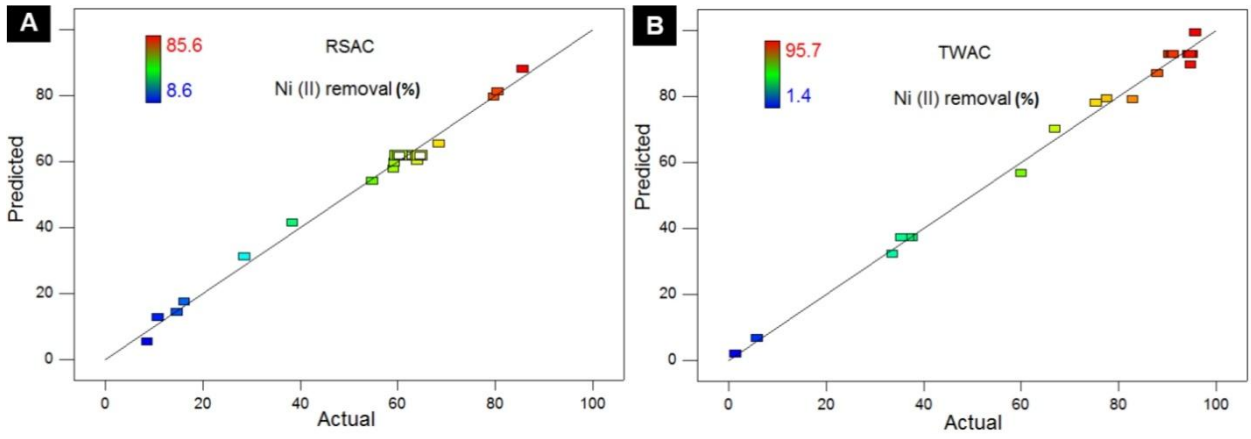

Figure 6: Actual versus predicted plot of regression models of RSAC (A) and TWAC (B).

Figure 7E and F shows the effects of pH of the solution (0.6 – 7.4), AC dosage (0.8 g/L – 9.2 g/L) and initial concentration of 50 ppm on the Ni^{2+} removal. Generally, investigated variables strongly influenced the percentage of Ni^{2+} removal. When adsorption process was employed at low values of AC dosage and pH of the solution, the removal of metal ions was almost undetected. However, simultaneous increasing of both factors led to increasing the removal efficiency of Ni^{2+} ion from aqueous solution. In detail, the maximum percentage of Ni^{2+} removal using RSAC was predicted 90 % at optimum *pH*–values of 7.0 and RSAC dosage of 6.0 g/L while the respective results for TWAC were 100 % at pH of 6.0 and TWAC dosage of 5.5 g/L. Moreover, model confirmation was also performed to search for the optimization conditions for all three variables, and its checked results were listed in Table 4. The predicted maximum percentage of nickel removals follow the order: RSAC (86.0 %) < TWAC (101.0 %). In verification experiments, the real removal efficiency using the *RSM*–based optimum conditions were found to be 80.3 % and 97.4 % for RSAC and TWAC mode, respectively. The experimental results, which were closed to the predicted values, indicating the suitability of the suggested models.

3.4. Adsorption studies

The graph plots of Langmuir, Freundlich, and Temkin isotherm were shown in Figure 8 and the respective model parameters were listed in Table 5. The obtained linear regression correlation and constant values illustrate that the experimental data were fitted to the proposed models. For the Langmuir isotherm, a plot of $1/C_e$ against $1/q_e$ produced a linear with the high R^2 value of 0.9972, 0.9347 for RSAC and TWAC, respectively. Moreover, the value of R_L was found by a variation between 0 and 1 confirmed that the adsorption of metal ions using various activated carbons is favorable under experimental conditions. Considering the Freundlich isotherm, the plot of $\log C_e$ against $\log q_e$ was employed to obtain the intercept K_F and slope n. The isotherm was fitted well by the Freundlich model with the R^2 value of 0.9994, 0.8245 model of RASC and TWAC, respectively. Note that constant values from the Temkin model were found to be lower R^2–values, 0.8839 and 0.7892 for RASC and TWAC, respectively. Generally, R^2–based adsorption isotherm models fit the data in the following order: Langmuir > Freundlich > Temkin. Langmuir models can, therefore, be used to assess the best description for Nickel adsorption behavior onto both activated carbons. On the other hand, values of maximum adsorption in the present study (q_m) were compared with previous works to recognize the close relationship between properties of ACs and adsorption capacities. Table 5 also indicates that tea waste–derived AC had approximately four–fold as much BET surface area as rice straw–derived activated carbon, and hence, the value of maximum adsorption capacity obtained 42.19 mg/g (TWAC) versus 21.23 mg/g (RSAC). The activated carbons used herein gave larger adsorption capacity results compared with some other activated carbons (Table 6). Thus, the use of rice straw and tea waste as abundant raw material to prepare AC for the promising Ni^{+2} removal from aqueous solutions.

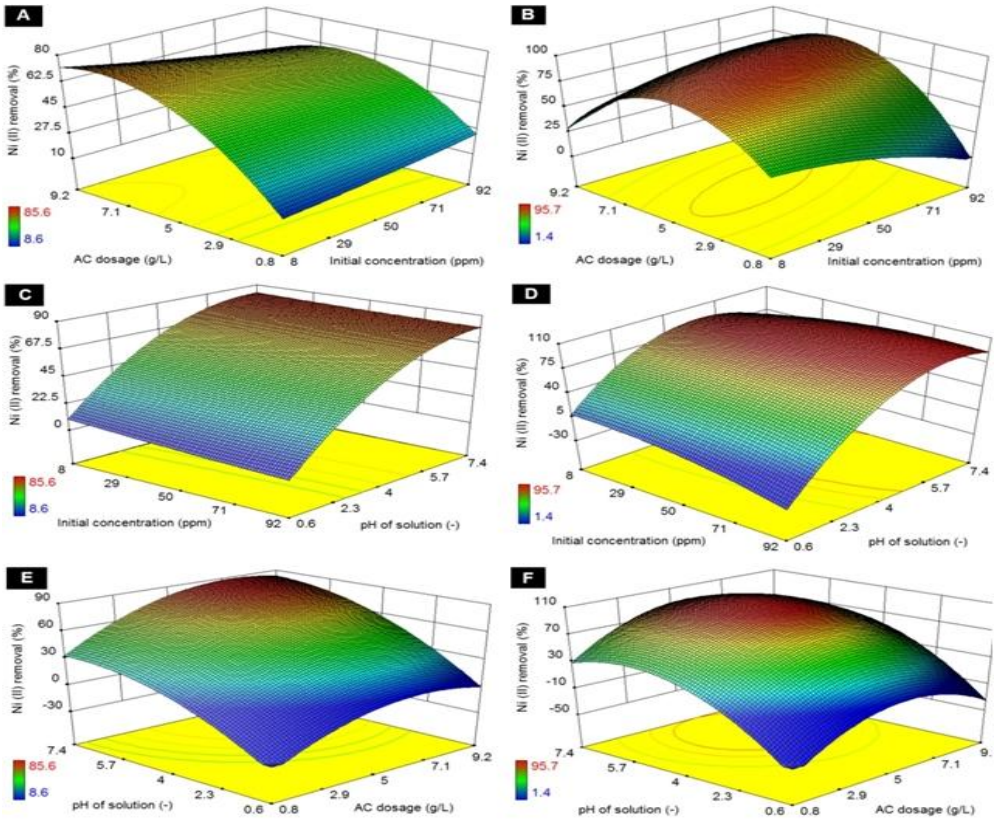

Figure 7: Effect of initial concentration, AC dosage and pH of solution = 4 on the Ni2+removal efficiency using RSAC (A) and TWAC (B); effect of initial concentration, pH of solution and AC dosage = 5 g/L on the Ni^{2+} removal efficiency using RSAC (C) and TWAC (D); effect of pH of solution, AC dosage and initial concentration = 50 ppm on the Ni^{2+} removal efficiency using RSAC (E) and TWAC (F).

Table 4: Model confirmation.

Sample	Concentration (ppm)	Dosage (g/L)	pH	Removal (%)	
				Predicted	Actual
RSAC	47.4	6.6	6.5	86.0	80.3
TWAC	89.0	5.6	6.3	101.0	97.4

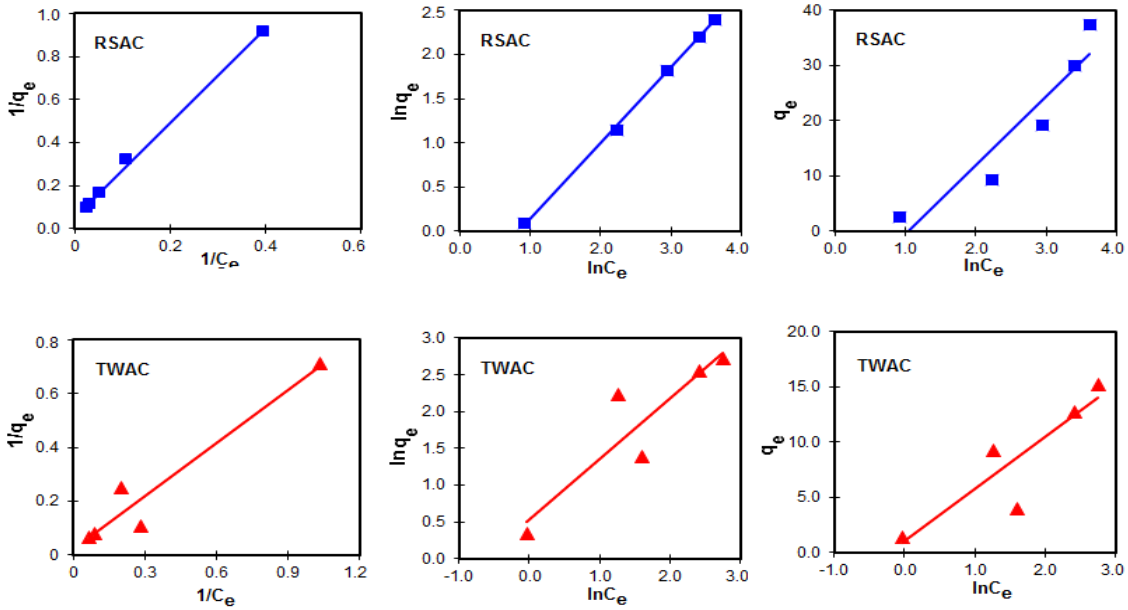

Figure 8: (Left to right) Langmuir, Preundlich and Temkin isotherm plots for adsorption of Ni^{2+} onto the RSAC and TWAC.

Table 5: Isotherm constants for AC models.

Langmuir isotherm	Adsorbent	K_L (L/mg)	q_m (mg/g)	R_L	R^2
	RSAC	0.0213	21.23	0.4839	0.9972
	TWAC	0.0361	42.19	0.3564	0.9347
Freundlich isotherm	Adsorbent	K_F [(mg/g).(L/mg)]$^{1/n}$	1/n		R^2
	RSAC	0.49	0.8572		0.9994
	TWAC	1.79	0.8181		0.8245
Temkin isotherm	Adsorbent	K_t (L/mg)	B_1		R^2
	RSAC	0.35	12.3990		0.8839
	TWAC	1.23	4.7162		0.7892

Table 6. Comparison of the textural properties of chemical-ACs and Ni^{2+} treatment

Source	Properties of AC			Ni^{2+} treatment				Ref
	Chemical agent	Activation temp.	S_{BET} (m^2/g)	C_o (ppm)	*D*osage (g/L)	pH	q_m (mg/g)	
Almond husk	H_2SO_4	700	-	25	5	5	4.87	[24]
Apricot	K_2CO_3	400	4.27	10	7	5.0	17.04	[25]
Palm shell	-	-	513	0.8	1	5	0.13	[26]
Glucose	H_3PO_4	450	698	60	0.6	7	48.5	[27]
Sucrose			460				42.4	
Starch			12				41.1	
Sugarcane fiber	NH_4Cl	500	836	147	10	7	10.3	[28]
Seed coat	H_3PO_4	300	-	40	5	7	13.51	[29]
Tea waste	KOH	700	-	47.4	6.6	6.5	21.23	*This work*
Tea waste	KOH	700	-	89.0	5.6	6.3	42.19	*This work*

Conclusion

The highly porous activated carbons fabricated from tea waste (TWAC) and rice straw (RSAC) were found to be an effective adsorbent for removal of Ni^{2+} ions from aqueous solution. By the optimization using the *RSM*–based quadratic regression equations, the impact of independent variables including metal ion concentration, pH and AC dosage on the removal of Ni^{2+} was statistically investigated. It is obvious that the derived quadratic models had both high fitness for the removal of nickel using RASC and TWAC. Accordingly, the maximum percentage of Ni^{2+} removal was 21.23 mg/g and 42.19 mg/g for RSAC and TWAC, respectively. The optimal adsorption conditions using RSAC were initial concentration of 47.4 ppm, AC dosage of 6.6 g/L and pH of 6.5 while those using TWAC were initial concentration of 89 ppm, AC dosage of 5.6 g/L and pH of 6.3.The results proved a great potential for application of low–cost agricultural waste–derived AC for remediation of environmental pollution like nickel contamination.

Acknowledgements-This research is funded by Foundation for Science and Technology Development Nguyen Tat Thanh University, Ho Chi Minh City, Vietnam; and a grant by the Korea Institute of Science and Technology (KIST) Institutional Program (Project No. 2Z04820-16-090), Seoul, Korea.

References

1. De Zuane J., in:, *Handb. Drink. Water Qual.*, John Wiley & Sons, Inc., Hoboken, NJ, USA, 2007, pp. 49–148.
2. Kandah, M.I., Meunier J.–L., *J. Hazard. Mater.* 146 (2007) 283.
3. Popuri S.R., Vijaya Y., Boddu V.M., Abburi K., *Bioresour. Technol.* 100 (2009) 194.
4. Hui K.S., Chao C.Y.H., Kot S.C., *J. Hazard. Mater.* 127 (2005) 89.

5. Farahani M., Abdullah S.R.S., Hosseini S., Shojaeipour S., Kashisaz M., *Procedia Environ. Sci.* 10 (2011) 203.
6. Aworn A., Thiravetyan P., Nakbanpote W., *J. Anal. Appl. Pyrolysis* 82 (2008) 279.
7. Kalderis D., Bethanis S., Paraskeva P., Diamadopoulos E., *Bioresour. Technol.* 99 (2008) 6809.
8. Kalderis D., Koutoulakis D., Paraskeva P., Diamadopoulos E., Otal E., del Valle J.O., Fernndez–Pereira C., *Chem. Eng. J.* 144 (2008) 42.
9. Maciá–Agulló J.A., Moore B.C., Cazorla–Amorós D., Linares–Solano A., *Carbon N. Y.*, 42, 1361 (2004).
10. Namasivayam C., Kadirvelu K., *Bioresour. Technol.* 62 (1997) 123.
11. Ahmadpour A., D.D. Do, *Carbon N. Y.* 34 (1996) 471.
12. Rodrguez–Reinoso F., Molina–Sabio M., *Carbon N. Y.* 30 (1992), 1111.
13. Lozano–Castelló D., Lillo–Ródenas M.A., Cazorla–Amorós D., Linares–Solano A., *Carbon N. Y.* 39 (2001) 741.
14. Caturla F., Molina–Sabio M., Rodroguez–Reinoso F., *Carbon N. Y.* 29 (1991) 999.
15. Guo Y., Rockstraw D.A., *Microporous Mesoporous Mater.*, 100, 12 (2007).
16. Olivares–Marín M., Fernández–González C., Macías–García A., Gómez–Serrano V., *Appl. Surf. Sci.*, 252, 5967 (2006).
17. Yagmur E., Ozmak M., Aktas Z., *Fuel* 87 (2008) 3278.
18. Byrne C.E., Nagle D.C., *Carbon N. Y.* 35 (1997) 259
19. Ping L., Gambier F., Brosse N., Wood adhesives from agricultural by–products: Lignins and tannins for the elaboration of particleboards, *Cellul. Chem. Technol.* 46 (7) (2012) 457
20. Sarnklong C., Cone J. W., Pellikaan W., Hendriks W. H., Utilization of Rice Straw and Different Treatments to Improve Its Feed Value for Ruminants: A Review, *Asian–Aust. J. Anim. Sci. Vol.* 23 (5) (2010) 680
21. Rahnama N., Ariff A. B. , Cellulase from rice straw, *BioResources* 8(2), (2013) 2881–2896
22. Liu H., Zhang J., Ngo H. H., Wu H., Cheng C., Guoa Z., Zhang C., *RSC Adv.* 5 (2015) 52048.
23. El–Sadaawy M., Abdelwahab O., *AEJ* 53 (2014) 399.
24. Ping L., Gambier F., Brosse N., Wood adhesives from agricultural by-products: Lignins and tannins for the elaboration of particleboards, *Cellul. Chem. Technol.* 46 (7) (2012) 457
25. Hasar H., Adsorption of nickel (II) from aqueous solution onto activated carbon prepared from almond husk, *J. Hazard. Mater.* 97 (2003) 49
26. Erdogan S., Onal Y., Iduygu G., Optimization of nickel adsorption from aqueous solution by using activated carbon prepared from waste apricot by chemical activation, *Appl. Surf. Sci.* 252 (2005), 1324
27. Onundi Y. B., Mamun A. A., Al Khatib M. F., Ahmed Y. M., Adsorption of copper, nickel and lead ions from synthetic semiconductor industrial wastewater by palm shell activated carbon, *Int. J. Environ. Sci. Tech.* 7 (2010) 751
28. Liu H., Zhang J., Ngo H.H., Wu H., Zhang C., Carbohydrates-based activated carbon with high surface acidity and basicity for nickel removal from synthetic wastewater ***RSC Adv.* 5** (2015) 52048
29. Ikhuoria E.U., Onojie O.C., Binding of nickel and zinc ions with activated carbon prepared from sugar cane fibre (saccharum officinarum L.), *Bull. Chem. Soc. Ethiop.* 21 (2007) 151